

Research Article

Optimization and Prediction of Concrete with Recycled Coarse Aggregate and Bone China Fine Aggregate Using Response Surface Methodology

Chandra Prakash Gour ¹, Priyanka Dhurvey ¹ and Nagaraju Shaik ²

¹Department of Civil Engineering, MANIT, 462003, Bhopal, India

²Department of Construction Technology and Management, Wollega University, Nekemte, Ethiopia

Correspondence should be addressed to Nagaraju Shaik; sknagaraju@wollegauniversity.edu.et

Received 19 August 2022; Revised 5 September 2022; Accepted 16 September 2022; Published 7 October 2022

Academic Editor: Samson Jerold Samuel Chelladurai

Copyright © 2022 Chandra Prakash Gour et al. This is an open access article distributed under the Creative Commons Attribution License, which permits unrestricted use, distribution, and reproduction in any medium, provided the original work is properly cited.

Construction recycled material is crucial for protecting natural resources and promoting sustainable human development in a rapidly industrializing world. Many administrations worldwide accepted that it is beneficial to use demolition waste in the concrete building industry to reduce manufacturing costs and minimize the use of virgin aggregates. However, control measures should be done as their mechanical properties are poorer than traditional aggregates. To overcome this problem, pozzolanic materials like bone china can be incorporated, providing extra CSH gel, which improves mechanical strength. Therefore, this research is aimed at producing eco-friendly concrete, which can be used for medium-grade strength, using recycled construction waste (RCA) as coarse and bone china fine aggregate (BCA) as fine aggregate. Workability, density, compressive, split tensile, and flexural strength are used to compare the fresh and hardened properties of the concrete. Experimental and statistical research is employed in the current study to evaluate the impact of RCA and BCA on the performance of concrete. To simulate all measurable responses, including workability, density, compressive, flexural, and split strength, RSM (response surface methodology) was utilized. The CCD (Central Composite Design) approach in RSM was used to create and analyze mixes in an experiment. Based on the experiment's results, mathematical models were designed and assessed using the analysis of variance test (ANOVA). The analysis of variance results demonstrated the statistical significance of each constructed model. Three-dimensional response surface plots created using established regression models were used to investigate the interaction between the respective variables and to optimize the mixing ratio. The results indicate that the optimum utilization of RCA is up to 40% and BCA up to 60% as coarse and fine aggregate replacement in concrete, respectively, which not only helps to reduce costs but also offers sustainability. Finally, it was concluded that the generated models might be employed by obtaining the maximum tested features of concrete to assure a quick mix design approach. To conduct the microstructure study, thin section techniques were used to observe a strong aggregate-matrix interaction.

1. Introduction

After water, concrete is the second most utilised substance in the world and is most usually used for construction. A fluid cement is used to bind fine and coarse particles in concrete (i.e., cement paste). Concrete needs aggregate between 60 and 75 percent of the volume [1]. Construction and demolition debris made of concrete, bricks, and tiles burden the city's few dumps [2]. However, recycled alternatives are required to fulfil industrial needs owing to a scarcity of nat-

ural resources for building materials [3]. From a sustainability perspective, using RCA in concrete is an inventive way to replace traditional natural aggregates. Due to the concrete industry's extensive use of natural resources, there are considerable losses in terms of money, energy, and the environment. It requires 40% energy, consumes 50% of all natural resources, and produces 50% of all waste [4].

Worldwide, ceramics have also been extensively used. However, the building and deconstruction of structures generate a significant amount of ceramic waste [5]. The annual

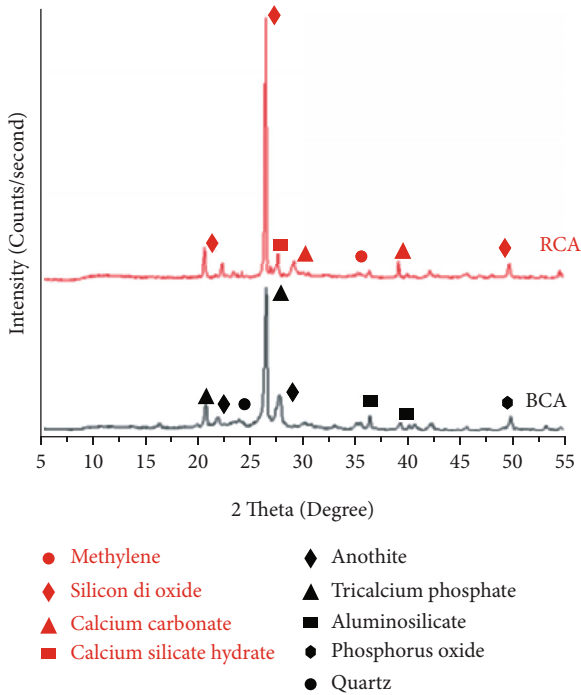


FIGURE 1: XRD of bone china aggregate and recycled coarse aggregate.

TABLE 1: Properties of BCA and RCA used in concrete mixes.

Properties	BCA	RCA
Maximum aggregate size	4.75 mm	20 mm
Fineness modulus	3.14%	6.53%
Grading zone	II	—
Specific gravity	2	3.2
Water absorption	3.2%	2.8%

production of bone china tableware in India is around 343,000 tonnes. In the same industrial sector, burnt bone china tableware goods make up 15%–20% of the entire production yet have few recycling alternatives. Usually, these wastes are disposed of in open dumping areas or landfills [6]. Although disposing of this ceramic waste demands a lot of landfill areas, it also poses a serious environmental danger. Groundwater contamination with ceramic powder can have serious adverse health effects [7]. In stores and factories, waste made of bone china is a vast problem that worsens yearly. Because producing concrete is less expensive, employing trash in the construction business is advantageous. But over the past several years, the quantity of waste bone china has steadily increased as more individuals utilise bone china products. Therefore, bone china garbage should not be disposed of in landfills since it cannot decompose organically. As a result, there is plenty of room for growth for bone china waste in the concrete building industry [6].

Bone china waste (BCW) is utilised in various proportions as a fine aggregate. The proper characteristic strength

is produced depending on the BCW substitution percentage, with a combination containing 60% BCW having the highest value. Concrete compressive, split tensile, and flexure strengths increased when fine bone china was used in place of fine aggregate. For low- to medium-rise buildings, BCW can be utilised as fine aggregate in structural concrete (up to 60 percent). This option is acceptable for use in moderately strong concrete as long as it satisfies the engineering specifications of the M20 grade concrete mix design. Thin section microscopy investigates the relationship between the microstructure and the bone china fine aggregate [8].

Rice husk ash was used to prepare the concrete mixture. Tests were conducted on specimens built from recycled concrete with different RHA levels and replacement ratios for coarse aggregate, workability, compressive strength, and splitting tensile strength. The results demonstrate that adding RHA reduces the workability and splitting tensile strength of the concrete while increasing its compressive strength. The findings also showed that the synergistic produced concrete made up of 30% RHA and 100% recycled coarse aggregate satisfies the design requirements for engineering applications and dramatically reduces the cost of creating concrete and carbon dioxide emissions [9, 10].

Costs associated with production will go down when waste is recycled to build concrete. Additionally, many governments worldwide have authorised the use of waste that has been destroyed in preventative measures for reuse as building aggregates to successfully reduce the usage of natural aggregates in concrete from ecological, technical, and commercial perspectives [11].

2. Research Significance

Makul et al., in their review paper, reported that all types of an aggregate made from demolished debris are composite materials made up of natural aggregate and cement mortar, and their mechanical properties are poorer than traditional aggregates. This is because of concrete degradation, which depends upon the entity of a filtering path across the interface between the bulk cement matrix and the particle assembly. To overcome this problem, they suggested adopting the durability measures given by National Concrete Standards, including the limit on maximum water to binder ratio and minimum cement content [12]. Additionally, Wang et al. proposed using various mixing techniques to include the pozzolanic ingredients, which quicken the carbonation process [13]. Research on FBCCA, i.e., fine bone china ceramic aggregate for the pozzolanic property, was conducted by Siddique et al. in 2019 and 2018, respectively. FBCCA further adds more CSH gel, which enhances mechanical characteristics and has structural uses [7, 14].

With this goal in mind, the authors completed the current study in concrete using RCA and BCA as fine and coarse aggregate replacements to create environmentally friendly concrete that may be utilised for medium-grade strength applications. The two-stage mixing technique, which Tam et al. developed as a new concrete mixing method, was used in several studies to examine the workability, compressive, flexural, and split tensile strengths of various mix combinations [15].

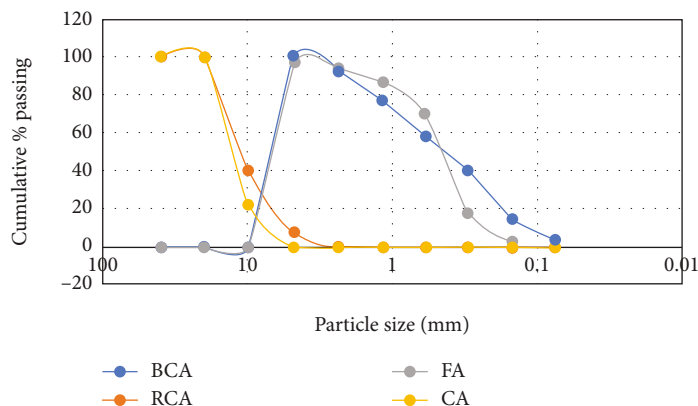


FIGURE 2: Particle size distribution curve for different aggregates.

TABLE 2: Mix proportions.

Mix	Cement (kg/m ³)	Natural sand (kg/m ³)	Bone china powder (kg/m ³)	Coarse aggregate (kg/m ³)	Recycled coarse aggregate (kg/m ³)
BOR0	494	840	0	1185	0
B20R0	494	672	168	1185	0
B40R0	494	504	336	1185	0
B60R0	494	336	504	1185	0
B80R0	494	168	672	1185	0
B100R0	494	0	840	1185	0
BOR20	494	840	0	948	237
BOR40	494	840	0	711	474
BOR60	494	840	0	474	711
BOR80	494	840	0	237	948
BOR100	494	840	0	0	1185
B40R40	494	504	336	711	474
B40R60	494	504	336	474	711
B60R40	494	336	504	711	474
B60R60	494	336	504	474	711
B100R100	494	0	840	0	1185

Some studies have been looking for the effective optimal design technique for the optimum parameters of various components. Response surface methodology (RSM) combines mathematical and statistical methods for modelling and data analysis in various engineering fields. In addition, RSM can model complicated multivariate processes, reduce the number of experimental trials, and show how response factor interactions affect optimization [16].

3. Experimental Program

3.1. Materials

3.1.1. Recycle Coarse Aggregate. The parent concrete for the RCA was M30 grade and was taken from the demolition site. In RCA, natural aggregate is bonded with old mortar. It comes

with a lightweight, porous mortar; recycled aggregate has lower specific gravity and density than natural aggregate. The X-ray Diffraction technique analysed RCA's mineralogical composition, as shown in Figure 1. The RCA properties are presented in Table 1.

3.1.2. Bone China Waste. The ingredients used to produce bone china include kaolin, feldspar, and bone ash. Concrete is produced using kaolin, a form of aluminium silicate that contains silicon dioxide and aluminium oxide. Figure 1 shows the results of an analysis of the mineralogical composition of BCA using the X-ray diffraction method. Table 1 provides the BCA property.

3.2. Sample Selection and Preparation. The unwanted noncementitious dirt was removed from RCA by washing. RCA and BCA materials were crushed in jaw crushers to create coarse and fine aggregate. An adjustment of the distance between the crusher's jaws was desired for RCA and BCA, and maximum aggregate size of 20 mm and 4.75 mm. The grading of the BCA, as fine aggregate, is done according to BIS 383 criteria (2016). Figure 2 displays the RCA and BCA particle size distribution curves.

3.3. Mixing Method and Mix Proportion. The present study used a novel concrete mixing method, the two-stage mixing strategy established by Tam et al., especially for concrete with RCA. In the initial mixing stage, the cement paste was created by combining all of the water, cement, and extra (if any) components, after which the recycled aggregates were added gradually to the cement slurry mix and constantly stirred for 10 minutes. Additional materials, including natural coarse particles and natural sand, were used in the second stage. The capabilities of RCA are improved by this method. The quantities of the concrete mix used in the experiment are displayed in Table 2. Under the directives of IS 10262: 2019 [17], the materials were mixed under the M30 grade mix design. In addition, 16 distinct combinations were created using an optimal water-to-binder ratio (w/b ratio) of 0.45. Coarse and fine aggregate was replaced with RCA and BCA in the following ratios: 0%, 20%, 40%, 60%, 80%, and 100%, respectively. The optimum percentage of RCA and BCA was found, and the combined effect of RCA and BCA in concrete was also examined.

TABLE 3: Experimental results.

Mix	Workability slump flow (mm)	Density of concrete (kg/m ³)	Compressive strength (N/mm ²)	Split tensile strength (N/mm ²)	Flexural strength (N/mm ²)
B0R0	73	2370	36.45	3.75	4.21
B20R0	66	2367	37.33	3.92	4.40
B40R0	54	2365	41.78	4.20	4.70
B60R0	47	2328	43.12	4.25	4.82
B80R0	44	2315	40.45	4.40	4.78
B100R0	36	2295	38.67	4.67	4.65
B0R20	69	2360	36.88	3.80	4.32
B0R40	62	2325	39.12	3.95	4.46
B0R60	58	2310	39.98	4.16	4.57
B0R80	48	2285	36.45	3.67	4.20
B0R100	39	2270	33.50	3.48	4.10
B40R40	43	2325	39.56	4.12	4.62
B40R60	39	2305	36.45	3.90	4.42
B60R40	34	2315	41.34	4.22	4.78
B60R60	28	2285	38.23	4.10	4.56
B100R100	26	2265	33.50	3.60	4.15

TABLE 4: ANOVA results for workability.

Source	DF	F value	p value	Significant
Model	5	80.42	0.001	Yes
<i>x</i>	1	144.76	0.001	Yes
<i>y</i>	1	114.21	0.001	Yes
<i>x</i> ²	1	15.93	0.003	Yes
<i>y</i> ²	1	0.18	0.677	No
<i>xy</i>	1	21.77	0.001	Yes

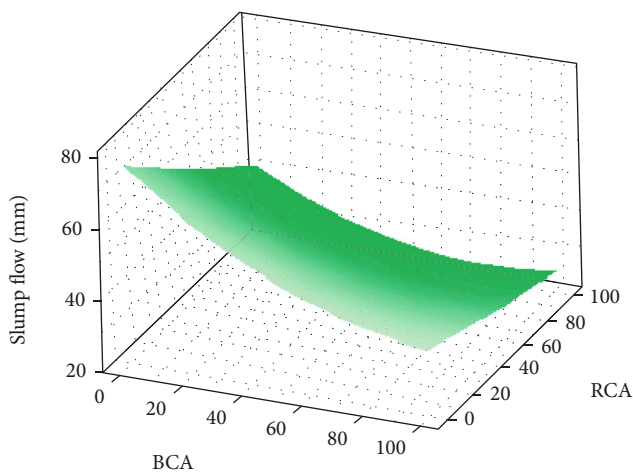


FIGURE 3: Response surface plot effect of BCA and RCA on workability.

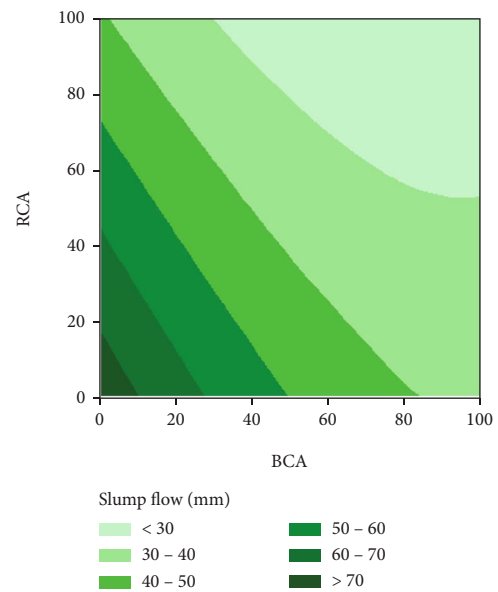


FIGURE 4: Contour plot for workability (slump test).

TABLE 5: ANOVA results for density of concrete.

Source	DF	F value	p value	Significant
Model	5	60.14	0.001	Yes
<i>x</i>	1	51.6	0.001	Yes
<i>y</i>	1	124.45	0.001	Yes
<i>x</i> ²	1	4.97	0.050	Yes
<i>y</i> ²	1	0.53	0.482	No
<i>xy</i>	1	37.85	0.001	Yes

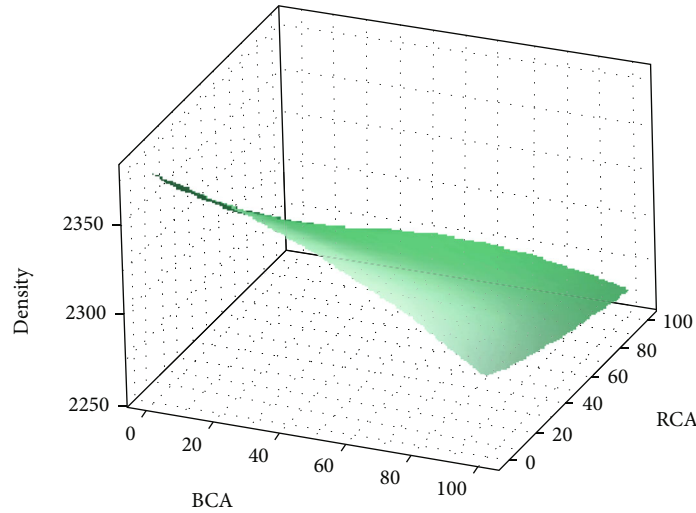


FIGURE 5: Response surface plot effect of BCA and RCA on density of concrete.

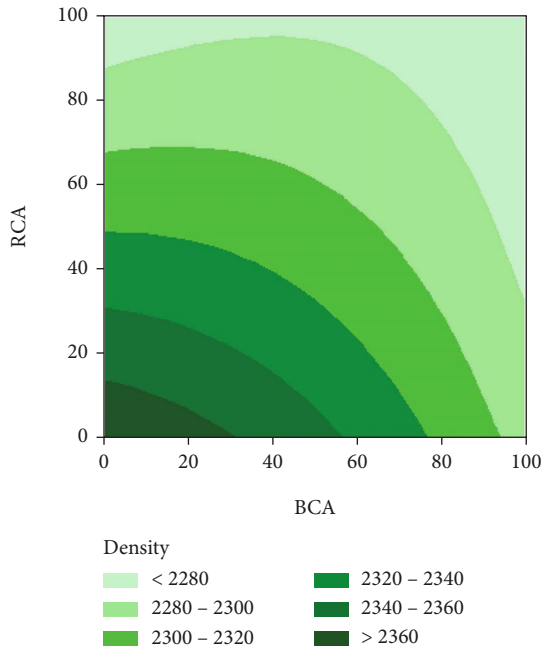


FIGURE 6: Contour plot for density of concrete.

TABLE 6: ANOVA results for compressive strength.

Source	DF	F value	p value	Significant
Model	5	8.72	0.002	Yes
x	1	1.05	0.331	No
y	1	2.73	0.129	No
x^2	1	14.96	0.003	Yes
y^2	1	7.76	0.019	Yes
xy	1	0.89	0.367	No

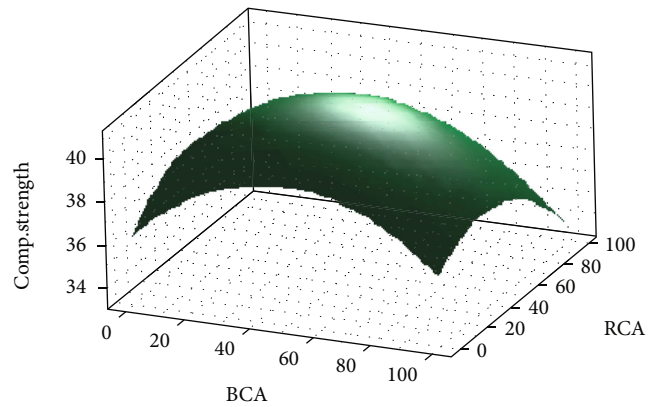


FIGURE 7: Response surface plot of the effect of BCA and RCA on compressive strength.

3.4. Experiment Design. Using correlations between input and output characteristics, the response surface method (RSM) is a mathematical approach for developing an empirical model. RSM is used in the current study's experiment, which is planned using a central composite method. The importance of each term and how each parameter and variable interacted with one another to affect each response in the models were determined using the analysis of variance (ANOVA). The coefficient of determination (R^2), F value, Lack of Fit, and p value were used to evaluate the effectiveness of the models. In the optimum regression model, R^2 was close to 1. The model may measure the relation between the response and each influencing variable and forecast the reaction if the ANOVA results show that it fits the data well. To display the interactions between the two test variables and the correlation between responses and experimental levels of each variable, three-dimensional (3D) surface plots of the regression model were plotted.

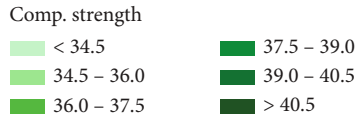
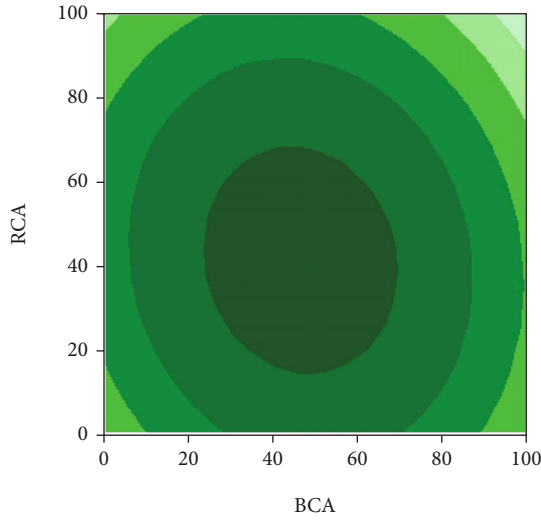


FIGURE 8: Contour plot for compressive strength.

TABLE 7: Confidence interval and probability interval.

Mix	95% confidence interval (95% CI)	95% probability interval (95% PI)
B0R0	(34.36, 38.13)	(32.84, 39.65)
B20R0	(36.86, 39.90)	(35.15, 41.60)
B40R0	(37.91, 40.96)	(36.21, 42.66)
B60R0	(38.00, 40.86)	(36.24, 42.61)
B80R0	(36.85, 39.85)	(35.13, 41.56)
B100R0	(33.75, 38.64)	(32.45, 39.94)
B0R20	(36.12, 39.16)	(34.42, 40.87)
B0R40	(36.75, 39.79)	(35.05, 41.50)
B0R60	(36.70, 39.56)	(34.95, 34.31)
B0R80	(35.71, 38.71)	(34.00, 40.43)
B0R100	(33.09, 37.97)	(31.78, 39.28)
B40R40	(39.85, 42.47)	(38.01, 44.05)
B40R60	(39.46, 42.19)	(37.65, 43.98)
B60R40	(39.59, 42.32)	(37.80, 44.11)
B60R60	(39.13, 42.00)	(37.38, 43.75)
B100R100	(30.64, 36.18)	(29.44, 37.38)

4. Results and Discussion

As indicated in Table 3, several design mixes investigated their fresh and hardened characteristics for compressive, flexural, and split tensile strength.

4.1. *Analysis of Workability.* The concrete’s slump value determines the consistency, flowability, compaction, and pumpability of a concrete mix. Investigations were done on how BCA and RCA affected the workability of concrete.

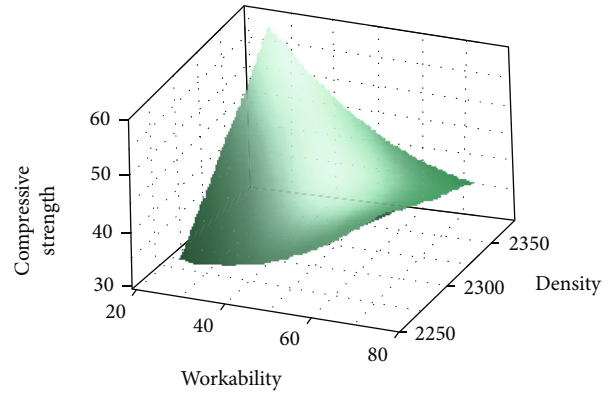


FIGURE 9: Response surface plot effect of workability and density on compressive strength.

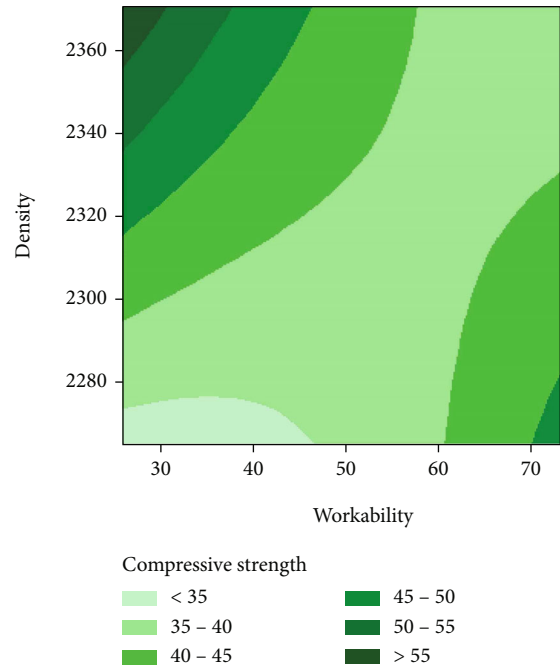


FIGURE 10: Counter plot of compressive strength w.r.t workability and density.

The outcome demonstrates that workability decreases as the ratio of RCA and BCA replacement increases because BCA and RCA absorb more water.

For construction engineers, a perfect workability forecast is essential and valuable. A regression-based study is carried out to predict the workability of concrete for various RCA and BCA percentages. Table 4 displays the ANOVA values for workability. The equation shows the regression models developed for workability in mm.

$$w = 76.62 - 0.6863x - 0.3883y + 0.002993x^2 + 0.000321y^2 + 0.002216xy, \tag{1}$$

where w is workability, x is BCA%, and y is RCA%.

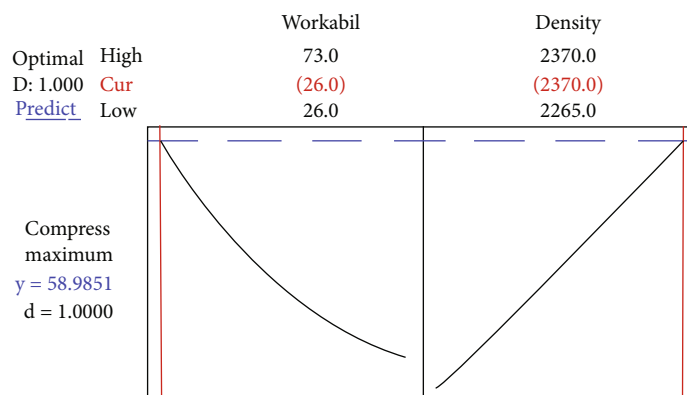


FIGURE 11: Maximum predicted value of compressive strength.

TABLE 8: ANOVA results for split tensile strength.

Source	DF	F value	p value	Significant
Model	5	22.97	0.001	Yes
x	1	28.77	0.001	Yes
y	1	57.86	0.001	Yes
x^2	1	0.84	0.380	No
y^2	1	17.47	0.002	Yes
xy	1	19.02	0.001	Yes

The determination coefficient $R^2 = 0.97$ and the adjusted coefficient $R^2 = 0.96$, all near 1 for the workability model, show that the regression model is suitable. A high degree of fitting was found by the “Lack of Fit p value” of 0.667, which was greater than 0.05 and indicated not significant. A model with p values less than 0.05 was considered significant.

The regression equation is graphically represented by the 3D response surface plots, as seen in Figure 3. To investigate the impacts of two parameters on the fresh properties, contour plots, as shown in figure 4, were plotted. In the contour plots, RCA values are shown on the y -axis, while BCA values are shown on the x -axis. The remaining factors were maintained at their midpoint values to create the contour plots since the statistical analysis considers two factors (i.e., BCA and RCA % replacement) to fluctuate between their low and high behaviour.

4.2. Analysis of Density. The density of hardened concrete was measured after 28 days. Table 3 shows that as the amount of BCA and RCA replacement increases, there is a minor drop in concrete density. Therefore, it is reasonable to state that the voids formed due to angularity will not significantly adversely affect other characteristics of hardened concrete because the most significant density drop is close to 4.43% with the B100R100 mix.

For construction engineers, a perfect workability forecast is essential and valuable. A regression-based study is carried out to predict the concrete density for the various mix. Table 5 displays the ANOVA values for density. The equation shows the regression models developed for density in

kg/m³.

$$d = 2376.88 - 0.389x - 1.235y - 0.00452x^2 + 0.00148y^2 + 0.00790xy, \quad (2)$$

where d is the density of concrete, x is BCA%, and y is RCA%.

The determination coefficient $R^2 = 0.96$ and the adjusted coefficient $R^2 = 0.95$, all near 1 for the workability model, show that the regression model is suitable. A high degree of fitting was found by the “Lack of Fit p value” of 0.482, which was greater than 0.05 and indicated not significant. A model with p values less than 0.05 was considered significant.

The regression equation is graphically represented by the 3D response surface plots, as seen in Figure 5. To investigate the impacts of two parameters on the density of the concrete, contour plots, as shown in Figure 6, were plotted. The contour plots display the RCA values on the y -axis and the BCA values on the x -axis. The remaining factors were maintained at their midpoint values to create the contour plots since the statistical analysis considers two factors (i.e., BCA and RCA % replacement) to fluctuate between their low and high behaviour.

4.3. Analysis of Compressive Strength. The compressive strength values as influenced by bone china aggregate (x) and recycled coarse aggregate (y) are shown in Table 3. Different proportions from combinations are considered in the design mix to optimize RCA and BCA replacement. The compressive strength results from different mixes. This happens due to unhydrated cement particles present in RCA, which react with water. So, we observed the improved property of concrete. Because of the increased specific surface of RCA, the two-stage mixing strategy improves the transition zone interface of recycled aggregates, enhancing the binding between new cement mortar and RCA, which is crucial to the behaviour of strength. Usage of RCA beyond 60% in concrete indicated a decrease in strength. The water content (i.e., w/b ratio) in the design mix becomes insufficient when the RCA ratio rises, slowing the hydration process. Based on compressive strength, the optimum value of RCA at 40%

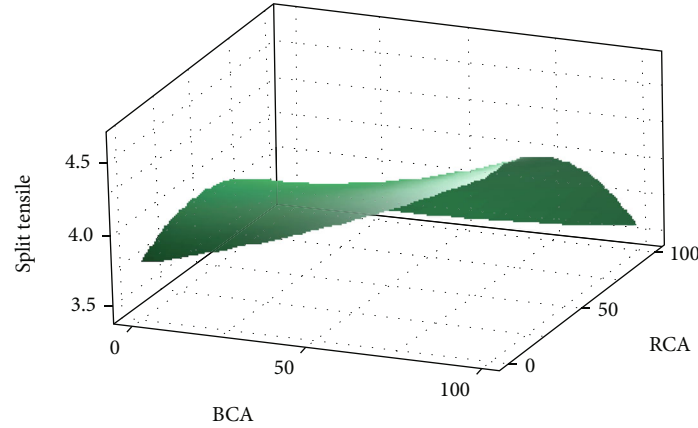


FIGURE 12: Response surface plot of the effect of BCA and RCA on split tensile strength.

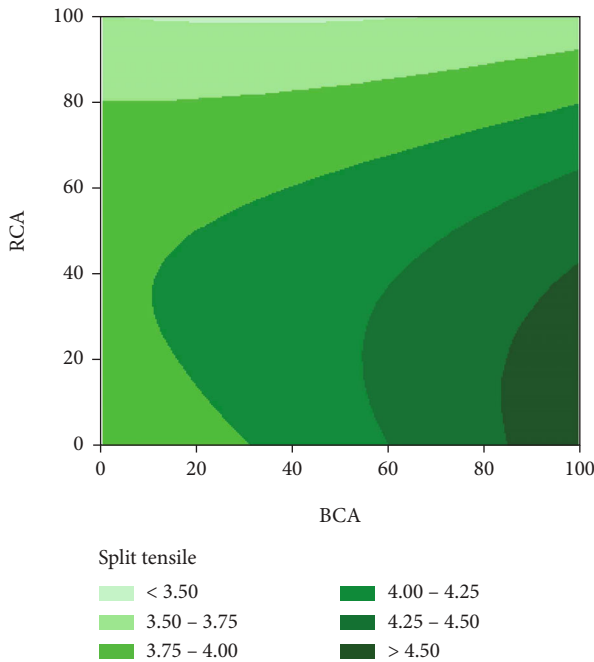


FIGURE 13: Contour plot for split tensile strength.

replacement with conventional coarse aggregate. Increased strength of up to 60% replacement was noticed due to the fine BCA's more outstanding production of CSH gel.

Furthermore, because it is fixed at 0.45, the water content in the design mix is insufficient beyond a 60% BCA ratio, leading to a poor hydration process. Low-density (lightweight) concrete has low compressive strength, and excessive water creates a weak interface zone. Based on the compressive strength aspect, the optimal BCA content for fine aggregate was determined to be 60%.

Table 6 displays the ANOVA values for compressive strengths. The equation shows the regression models developed for 28-day compressive strength.

$$F_{cs} = 36.249 + 0.1333x + 0.0892y - 0.001338x^2 - 0.000964y^2 - 0.000207xy, \quad (3)$$

where F_{cs} is compressive strength, x is BCA%, and y is RCA%.

The determination coefficient $R^2 = 0.8135$ and the adjusted coefficient $R^2 = 0.7202$, all near 1 for the compressive strength model, show that the regression model is suitable. A high degree of fitting was found by the "Lack of Fit p value" of 0.331, 0.129, and 0.367, respectively, which was greater than 0.05 and indicated not significant. A model with p values less than 0.05 was considered significant.

As seen in Figure 7, the regression equation is graphically represented by the 3D response surface plots. To investigate the impacts of two parameters on the mechanical performance of the concrete, contour plots, as shown in Figure 8, were plotted. The y -axis of the contour plots represents RCA values, while the x -axis represents BCA values. The remaining factors were maintained at their midpoint values to create the contour plots since the statistical analysis considers two factors (i.e., BCA and RCA % replacement) to fluctuate between their low and high behaviour. Table 7 shows the confidence interval and probability interval plot for various mixes.

4.4. Relationship between Workability, Density, and Compressive Strength of Different Mixes.

The experimental results found a correlation between compressive strength with density and workability, as illustrated in the equation below. Graphs of the regression equation are shown in the 3D response surface plots. Figure 9 shows how workability and density affect the compressive strength determined from the established equations. Contour plots, as shown in figure 10, were generated to study the effects of two factors on the compressive strength performance of the concrete.

$$F_{cs} = -252 + 16.3w - 0.17d + 0.00763w^2 + 0.00013d^2 - 0.00741wd, \quad (4)$$

where F_{cs} is the compressive strength of concrete, d is the density of concrete in kg/m^3 , and w is workability in mm.

The determination coefficient $R^2 = 0.81$ and the adjusted coefficient $R^2 = 0.71$, all near 1 for the model, show that the regression model is suitable.

TABLE 9: ANOVA results for flexural strength.

Source	DF	F value	p value	Significant
Model	5	10.79	0.001	Yes
x	1	5.69	0.038	Yes
y	1	18.10	0.002	Yes
x^2	1	3.65	0.085	No
y^2	1	6.26	0.031	Yes
xy	1	5.74	0.038	Yes

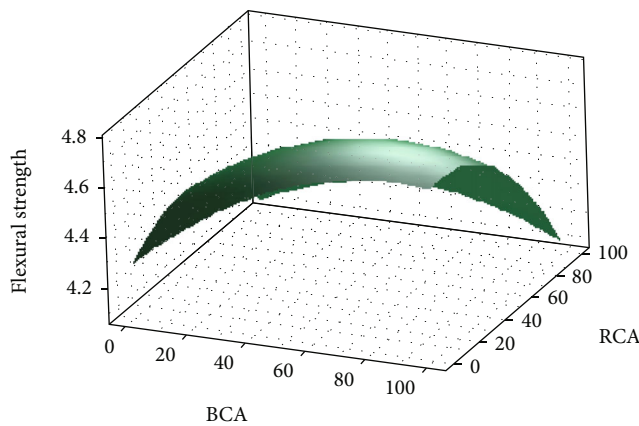


FIGURE 14: Response surface plot of the effect of BCA and RCA on flexural strength.

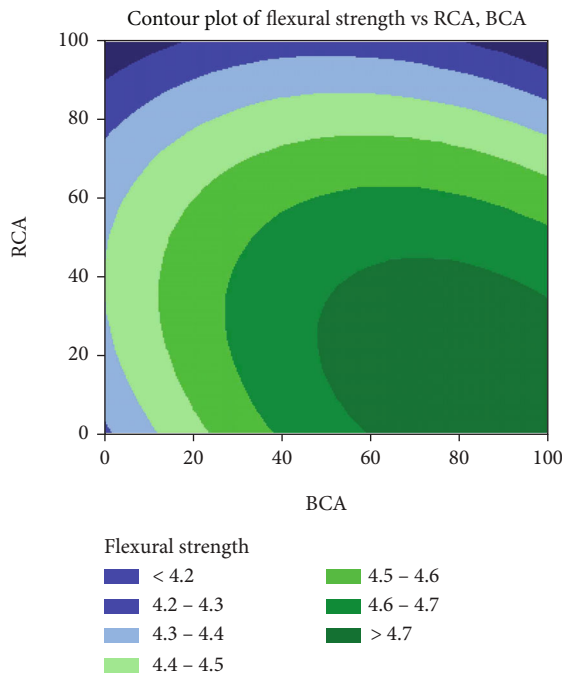


FIGURE 15: Contour plot for flexural strength.

According to Figure 11, the maximum compressive strength at 26 mm slump and 2370 kg/m³ density is predicted to be 58.98 N/mm².

4.5. *Analysis of Split Tensile Strength.* The tensile strength of each design combination was evaluated using a cylindrical specimen with dimensions of 150 mm in diameter and 300 mm in height. Despite being less than compressive strength, split tensile strength is essential for determining the viability of constructions; in various combinations, as indicated in Table 3.

Table 8 displays the ANOVA values for split tensile strengths. The equation shows the regression models developed for 28-day split tensile strength.

$$F_s = 3.7789 + 0.00619x + 0.00951y - 0.000027x^2 - 0.000123y^2 - 0.000081xy, \tag{5}$$

where F_s is split tensile strength, x is BCA%, and y is % RCA%.

The determination coefficient $R^2 = 0.92$ and the adjusted coefficient $R^2 = 0.88$, all near 1 for the split tensile strength model, show that the regression model is suitable and well fitted. The F -test showed that the model was very significant, with low p values and a high F value of 22.97, 28.77, and 57.89. Table 8 also shows that all of the model terms' p values were less than 0.05, suggesting that they were all capable of having a considerable impact on concrete's split tensile strength.

Graphs of the regression equation are shown in the 3D response surface plots. Figure 12 shows how BCA and RCA affect the split tensile strength determined from the established equations. As shown in figure 13, contour plots were produced to examine the effects of two factors on the concrete's split tensile strength performance.

4.6. *Analysis of Flexural Strength.* Testing the concrete's flexural strength determines how well it resists bending stresses. A 100 × 100 × 500 mm beam specimen was used to compare the M30 grade of concrete to all other mixes to ascertain the average flexural strength. This study looked at the flexural strength of various RCA and BCA cylinder specimen combinations on the 28th day after curing, as indicated in Table 3.

Table 9 displays the ANOVA values for flexural strengths. The equation shows the regression models developed for 28-day flexural strength.

$$F_f = 4.2807 + 0.01062x + 0.00612y - 0.00006x^2 - 0.000078y^2 - 0.000047xy, \tag{6}$$

where F_f is flexural strength, x is BCA%, and y is RCA%.

The determination coefficient $R^2 = 0.84$ and the adjusted coefficient $R^2 = 0.76$, all near 1 for the split tensile strength model, show that the regression model is suitable. A small p value ($<.05$) indicates a more significant substantial influence on the model's relevant response variance for each term. As noted in Table 9, the model, x, y, y^2 , and xy

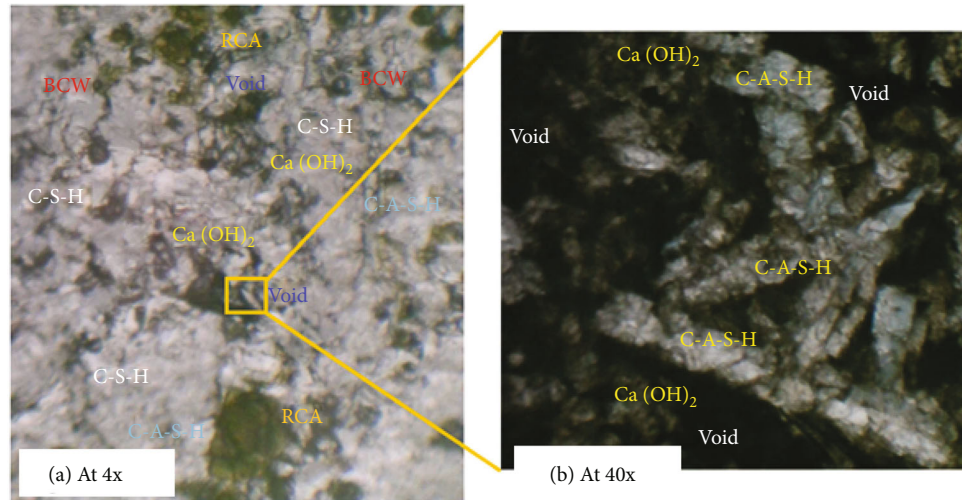


FIGURE 16: Microstructure of B60R40 mix.

parameters are significant since the p value is less than .05. But χ^2 had no appreciable impact on flexural strength.

The regression equation is graphically represented by the 3D response surface plots. Figure 14 shows how BCA and RCA affect the flexural strength determined from the established equations. Contour plots, as shown in Figure 15, were plotted to analyze the influence of two factors on the flexural strength performance of the concrete.

5. Microstructure Analysis

Thin-section microscopy is used for the analyses of concrete microstructure with coarse RCA and fine BCA. Presently, a variety of thin-section techniques are accessible, with polarizing and scanning electron microscopes being two well-known geological methods. To study concrete, the same methodologies have been expanded and enhanced. They are unique as they offer insights into the mineralogical, chemical, and microstructural characteristics of different materials and, as a result, provide a scientific basis for understanding that allows the evaluation of concrete's physical and mechanical behaviour. A thin section sample of Mix B60R40 after 28 days was prepared. The strength of Mix B60R40 is the highest as it provides extra CSH gel formation, as shown in Figure 16. The significant portion constitutes C-S-H, i.e., calcium sulfoaluminate hydrates around 70-75%, providing the strength for B60R40 mix. $\text{Ca}(\text{OH})_2$ and C-A-S-H, i.e., ettringite, constitute about 20% and 7%, respectively, after 28 days, as shown in Figure 16(b) at 4x magnification. Calcium hydroxide, $\text{Ca}(\text{OH})_2$, are not clearly visible because fragments of residual clinker (due to RCA) may be obscured in the thickness of the thin section.

6. Conclusions

The use of RCA as the coarse aggregate and BCA as the fine aggregate in place of natural aggregates in concrete was examined in this study. The individual impacts of RCA and BCA were first investigated to determine the optimal values. The experimental workability, compressive, flexural,

and split tensile strength data at various percentages of RCA and BCA were then used to create the response surface method. Based on the data and discussion, the following conclusions may be drawn.

- (i) More water is required to achieve the specified workability since the workability of concrete decreases as RCA and BCA levels increase
- (ii) With bone china aggregate and recycled coarse aggregate, the RSM showed an effective method for improving the characteristics of concrete
- (iii) All of the generated regression models for split tensile, flexural, and compressive strength at 28 days were statistically significant at a 95% confidence level
- (iv) With 60% BCA replaced with fine aggregate, the compressive strength increased by 18.3%, and when 60% RCA was used as coarse aggregate, the compressive strength improved by 9.68%. The optimum value was obtained with 60% BCA and 40% RCA; compared to normal concrete, an increase in compressive strength was observed by 13.41%. The strength properties of BCA are improved by its pozzolanic behaviour, which also meets the characteristic strength requirements for concrete
- (v) All replacement mixes meet the tensile strength criterion since their tensile strengths range from 3 to 5 N/mm^2 . Compared to normal concrete, an increase in tensile strength was observed by 12.5% and 4.5%, respectively, with a ratio of 40-60 and 60-40 of RCA and BCA
- (vi) An increase in flexure strength was observed by 3.91% and 10.32%, respectively, with a ratio of 60-40 and 60-60 of RCA and BCA, compared to normal concrete. All replacement mixes' flexural strengths meet the I.S. criteria for M30 grade

- (vii) With RCA and BCA, a two-stage mixing process improves the characteristics of concrete. Cement slurry increases the bonding between waste aggregates and new concrete mortar, which is reflected in improved compressive, tensile, and flexure strength values
- (viii) Proposed prediction models of compressive, split tensile, and flexure strength are reliable for predicting strength at 20, 40, 60, 80, and 100% of RCA and BCA content in concrete
- (ix) RCA and BCA can be used in structural concrete as coarse and fine aggregate (up to 60%). This alternative may be utilised in concrete of moderate strength because it fulfils the engineering specifications for the M30 grade mix design for concrete

Data Availability

The data used to support the findings of this study are included within the article.

Conflicts of Interest

There is no conflict of interest among the authors.

References

- [1] S. H. Kosmatka and M. L. Wilson, *Design and control of concrete mixtures: the guide to applications, methods, and materials*, Portland Cement Association, 2011.
- [2] H. Duan and J. Li, "Construction and demolition waste management: China's lessons," *Waste Management & Research: The Journal for a Sustainable Circular Economy*, vol. 34, no. 5, pp. 397–398, 2016.
- [3] J. Han and J. K. Thakur, "Sustainable roadway construction using recycled aggregates with geosynthetics," *Sustainable Cities and Society*, vol. 14, pp. 342–350, 2015.
- [4] N. D. Oikonomou, "Recycled concrete aggregates," *Cement and Concrete Composites*, vol. 27, no. 2, pp. 315–318, 2005.
- [5] L. G. Li, Z. Y. Zhuo, J. Zhu, J. J. Chen, and A. K. H. Kwan, "Reutilizing ceramic polishing waste as powder filler in mortar to reduce cement content by 33% and increase strength by 85%," *Powder Technology*, vol. 355, pp. 119–126, 2019.
- [6] S. Siddique, S. Shrivastava, S. Chaudhary, and T. Gupta, "Strength and impact resistance properties of concrete containing fine bone china ceramic aggregate," *Construction and Building Materials*, vol. 169, pp. 289–298, 2018.
- [7] S. Siddique, S. Shrivastava, and S. Chaudhary, "Durability properties of bone china ceramic fine aggregate concrete," *Construction and Building Materials*, vol. 173, pp. 323–331, 2018.
- [8] C. P. Gour, P. Dhurvey, and N. Shaik, "Design of structural concrete with bone China fine aggregate using statistical approach," *Advances in Materials Science and Engineering*, vol. 2022, Article ID 6244768, 12 pages, 2022.
- [9] C. Liu, W. Zhang, H. Liu et al., "Recycled aggregate concrete with the incorporation of rice husk ash: mechanical properties and microstructure," *Construction and Building Materials*, vol. 351, article 128934, 2022.
- [10] P. Verma, P. Dhurvey, and V. P. Sundramurthy, "Structural behaviour of metakaolin geopolymer concrete wall-type abutments with connected wing walls," *Advances in Materials Science and Engineering*, vol. 2022, Article ID 6103595, 10 pages, 2022.
- [11] S. F. U. Ahmed, "Existence of dividing strength in concrete containing recycled coarse aggregate," *Journal of Materials in Civil Engineering*, vol. 26, no. 4, pp. 784–788, 2014.
- [12] N. Makul, R. Fediuk, M. Amran et al., "Use of recycled concrete aggregates in production of green cement-based concrete composites: a review," *Crystals (Basel)*, vol. 11, no. 3, p. 232, 2021.
- [13] R. Wang, N. Yu, and Y. Li, "Methods for improving the microstructure of recycled concrete aggregate: a review," *Construction and Building Materials*, vol. 242, article 118164, 2020.
- [14] S. Siddique, S. Shrivastava, and S. Chaudhary, "Influence of ceramic waste on the fresh properties and compressive strength of concrete," *European Journal of Environmental and Civil Engineering*, vol. 23, no. 2, pp. 212–225, 2019.
- [15] V. W. Y. Tam and C. M. Tam, "Diversifying two-stage mixing approach (TSMA) for recycled aggregate concrete: TSMA_s and TSMA_{sc}," *Construction and Building Materials*, vol. 22, no. 10, pp. 2068–2077, 2008.
- [16] F. Sabbagh, I. I. Muhamad, Z. Nazari, P. Mobini, and S. B. Taraghdari, "From formulation of acrylamide-based hydrogels to their optimization for drug release using response surface methodology," *Materials Science and Engineering: C*, vol. 92, pp. 20–25, 2018.
- [17] I. Bis, *10262–2019 (2019) Specification for mix design guidelines for concrete*, Bureau of Indian Standards, New Delhi, 2019.